Vol. 194: 75–85, 2000 | MARINE ECOLOGY PROGRESS SERIES
Mar Ecol Prog Ser | Published March 17

A microsensor study of light enhanced Ca^{2+} uptake and photosynthesis in the reef-building hermatypic coral *Favia* sp.*

Dirk de Beer[1,], Michael Kühl[2], Noga Stambler[3], Lior Vaki[3,†]**

[1]Max Planck Institute for Marine Microbiology, Celsiusstraße 1, 28359 Bremen, Germany
[2]Marine Biological Laboratory, University of Copenhagen, Strandpromenaden 5, 3000 Helsingør, Denmark
[3]Department of Life Sciences, Bar Ilan University, Ramat Gan 52900, Israel

ABSTRACT: The coupling between CO_2 and Ca^{2+} exchange and photosynthesis by corals (*Favia* sp.) was studied with microsensors for Ca^{2+}, O_2, pH and CO_2. The profiles of these compounds, measured perpendicular on the coral surface, were strongly influenced by light. During illumination, the concentration of O_2 and the pH at the polyp surface was higher than in the surrounding seawater, while the concentrations of Ca^{2+} and CO_2 were lower. In the dark the inverse was observed. Furthermore, simultaneous recording of concentration changes at the coral surface, in response to light and inhibitors, were performed with pairs of the sensors. The concentration changes of CO_2 and pH were slow, while those of Ca^{2+} and O_2 were immediate and fast. The concentration changes of the O_2 and Ca^{2+} concentrations at the coral surface were synchronous in response to changes in light conditions and to inhibition of the photosynthesis. Also, the spatial distribution of photosynthetic activity over a single polyp coincided with the distribution of Ca^{2+} concentration changes. These results show that Ca^{2+} dynamics at the polyp surface is not an indirect effect of increased $CaCO_3$ precipitation at the skeleton, but indicates the presence of a Ca^{2+} uptake mechanism that is directly correlated to photosynthesis. Inhibition of carbonic anhydrase strongly decreased photosynthesis, especially at higher light intensities. This, combined with the observed increase in CO_2 concentration changes and absolute increase in CO_2 concentration at the tissue surface, demonstrated the importance of carbonic anhydrase for CO_2/DIC uptake and transport to the site of photosynthesis.

KEY WORDS: Calcification · Coral · Microsensors · Photosynthesis · Inhibitors

INTRODUCTION

The phenomenon of 'light enhanced calcification' (Goreau & Goreau 1959) by hermatypic corals is well-documented (Barnes & Chalker 1990, Marshall 1996a). However, the importance of the interrelation of photosynthesis and calcification in corals is still debated (Carlon 1996, Goreau et al. 1996, Marshall 1996b), and the mechanisms of the coupling are poorly understood (Crossland & Barnes 1974, McConnaughey 1987, Barnes & Chalker 1990). All hermatypic corals are symbioses between coral hosts and dinoflagellate algal symbionts, often called zooxanthellae. Calcification in hermatypic corals is coupled to photosynthesis, since it is strongly reduced by shading and exposure to dichlorophenyl dimethyl urea (DCMU) (VanderMeulen et al. 1972, Ip & Krisnaveni 1991), a strong inhibitor of photosystem II. Generally, in hermatypic corals, the molar rate of calcium precipitation is of the same order of magnitude as the photosynthetic production of oxygen (McConnaughey 1994). However, it is also reported that calcification rates by corals are less than 50% of their photosynthesis rates, even lower on the reef community level (Gattuso et al. 1999). Precipitation of calcium carbonate reduces the alkalinity, lowers the pH and increases the CO_2 concentration (McConnaughey 1987). As a result, calcification can balance the changes in pH and CO_2 concentration induced by photosynthesis. It is hypothesized that in the

*This paper is dedicated to Lior Vaki, who died in a tragic accident during the time of this study
**E-mail: dbeer@mpi-bremen.de
†Deceased

green alga *Chara* (McConnaughey 1991) and in foraminifera (Erez 1983) calcification enhances photosynthesis by reducing alkalinity and increasing the availability of CO_2. This seems not the case for corals, as inhibition of calcification does not reduce photosynthesis (Yamashiro 1995). Nevertheless, elevated CO_2 levels increased photosynthesis but decreased calcification (Gao et al. 1993). It is thought that the decreased pH due to CO_2 addition is not balanced by the increased photosynthesis and that the concomitantly decreased over-saturation of calcium carbonate makes it more difficult for the corals to calcify (Pennisi 1998).

In corals calcification is a complex process, involving uptake at the tissue surface, transport through the tissue and secretion at the skeleton side (Barnes & Chalker 1990, Muscatine et al. 1997). Calcification and photosynthesis are spatially separated, as the zooxanthellae are usually located close to the polyp surface. The existence of external and internal gradients forms a further complication (Kühl et al. 1995). Exchange of solutes with the surrounding seawater occurs through the diffusive boundary layer adjacent to the polyp surface, whose thickness depends on the hydrodynamics near the coral (Patterson 1992, Shashar et al. 1993). Consequently, solute concentrations at the polyp surface can differ considerably from those in the surrounding seawater.

Our aim was to study the relation between calcium exchange at the polyp surface, photosynthesis and respiration, and to unravel the mechanism of a possible coupling between these processes, by using microsensors for the main solutes involved: O_2, CO_2, Ca^{2+} and H^+. Microsensors have sufficient spatial resolution to measure at the very surface of the tissue, with minimal disturbance of the polyp and its microenvironment (Revsbech & Jørgensen 1986). Due to the high spatial and temporal resolution of microsensor measurements, and since photosynthesis is located near the coral surface, we were able to study photosynthesis and calcium uptake simultaneously.

MATERIAL AND METHODS

Collection and incubation of corals. Experiments were done with *Favia* sp. colonies, as previous experiments demonstrated their suitability for microsensor studies (Kühl et al. 1995). The individual polyps had a diameter of ca 1 cm, the mouth opening was in the middle of a central cavity with a diameter of ca 0.3 to 0.7 cm and a depth of 0.1 to 0.5 cm. The variation in depth reflects the flexibility of the polyps that continuously change their shape. A rim of tissue, from which at night 0.5 cm long tentacles are extended, surrounded the central cavity. A complete description of the polyp structure has been given previously (Kühl et al. 1995). Small colonies (ca 5 cm in diameter) were obtained from a platform at 5 m depth by SCUBA diving in the Gulf of Aquaba (Eilat, Israel). After collection, the colonies were stored in tanks at the shore and continuously flushed with fresh seawater. Experiments were performed within 7 d after collection. For laboratory experiments, the corals were placed in a flow cell through which seawater was pumped from a continuously aerated recirculation tank. The recirculation tank contained 80 l of seawater that was replaced daily. The temperature during experiments was 24°C, equaling the ambient seawater temperature. Microsensor measurements lasted less than 16 h after which the colonies were allowed to recover in the dark for at least 8 h. The light source was a fiber optic halogen lamp (Schott KL1500, Germany). Incident light intensity was quantified as down-welling scalar irradiance with a Biospherical Instruments meter (QSL-100, USA).

Microsensors. Ca^{2+} microsensors were prepared as described previously (Ammann et al. 1987), but with a 10 mM $CaCl_2$ solution as filling electrolyte. The Ca^{2+} sensors were shielded against electrical noise (Jensen et al. 1993) and painted black up to 20 µm from the tip. The microsensor shafts were wrapped in aluminum foil, to avoid possible side effects from light and temperature. Calibration was performed in NaCl solutions (40 g l^{-1}), with 1 to 20 mM $CaCl_2$. The Ca^{2+} sensors were insensitive to pH and O_2. Fast responding O_2 microsensors and full glass pH microsensors were prepared as described previously (Revsbech & Jørgensen 1986, Revsbech 1989). CO_2 microsensors were prepared and calibrated as described previously (de Beer et al. 1997), and were also painted black and wrapped in aluminum foil. The Ca^{2+} and O_2 sensors had response times (t_{90}) of <1 s, the CO_2 and pH sensors of <10 s.

All sensors were applied as described previously (Kühl et al. 1995); however, for this study microsensor measurements were restricted to the polyp surface or the boundary layer. An electronic shutter (Vincent Associates), inserted into the light path between lamp and sample, was used for fast and reproducible darkening of the coral. The concentration dynamics at the polyp surface were recorded simultaneously with 2 different microsensors positioned at the polyp surface, with their measuring tips <100 µm apart. The 2 microsensors were positioned by 2 micromanipulators, placed on opposite sides of the aquarium, at an angle of 17°. The light source was positioned in between the sensors directly above the polyp. Unless stated otherwise, these measurements were done near the top of the inner rim (see also Kühl et al. 1995).

Gross photosynthetic rates were determined with O_2 microsensors by the light-dark shift method (Revsbech

& Jørgensen 1983), as the initial rate (<1 s) of O_2 depletion after darkening. A delay of O_2 depletion was interpreted as a sign that the sensor was not perfectly positioned at the surface. Then the readings were discarded and the sensor was repositioned until the response was immediate. More details of the method are presented elsewhere (Revsbech & Jørgensen 1983, Glud et al. 1992, Kühl et al. 1995).

Profiles were measured by positioning the microsensors using a motorized micromanipulator (Märtzhäuser, LOT-ORIEL, Germany). The sensors were manipulated at an angle of 17° relative to the incident light. The surface of the polyp was the reference point (depth = 0), determined with a dissection scope. Negative depths indicate positions above the surface. The oxygen distribution above a single polyp was determined by measuring an array of profiles along a transect through the center of the polyp. From these data, 2-D contour plots were generated using SURFER 5.03 (Golden Software, Inc., Colorado, USA), by a Kriging routine with linear interpolation.

Diffusion coefficients. We used literature values for the diffusion coefficient of O_2 and Ca^{2+} in seawater at 24°C corrected for temperature and type of counter ion (Broecker & Peng 1974, Li & Gregory 1974); the diffusion coefficient of O_2 is 2.24×10^{-9} m^2 s^{-1}, the self-diffusion coefficient of Ca^{2+} is 0.79×10^{-9} m^2 s^{-1}, the diffusion coefficient of Ca^{2+}, with HCO_3^- as counter ion, was calculated to be 0.95×10^{-9} m^2 s^{-1}.

Inhibitors. Ruthenium-red, an inhibitor of Ca-ATPase (Marshall 1996a), was added to final concentrations of 20 to 100 µM. Ethoxyzolamide, an inhibitor of carbonic anhydrase that can penetrate into cells, was dissolved in dimethyl sulfoxide (DMSO) and added to a final concentration of 1 mM (Tambutte et al. 1995). The final DMSO concentration was 0.1%. DCMU, a strong inhibitor of photosystem II, was dissolved in ethanol and added to final concentrations of 0.5 and 2.5 µM (Ip & Krisnaveni 1991). Fresh colonies were used for each experiment with inhibitors.

RESULTS

Experimental problems

As pointed out previously (Kühl et al. 1995), corals exhibit some special features that made microsensor measurements rather difficult and required frequent observation of the measuring position by a dissection microscope. Sudden stimuli, e.g. by touching the polyp surface with microsensor tips or by abrupt changes in light intensity, often resulted in contraction of the coral tissue. Prolonged incubation in the dark resulted in expansion of the tissue and extension of the tentacles, therefore only a few dark profiles were measured. Furthermore, polyps excreted large amounts of mucus under stress, e.g. after incubation in the light for more than 16 h and occasionally after addition of inhibitors of carbonic anhydrase. Addition of the other inhibitors did not result in mucus formation. The mucus formed an additional barrier for substrate exchange, resulting in changes in the surface concentrations. Mucus coating the measuring tip could also directly reduce the response of the O_2 sensors. Experiments influenced by mucus formation were discarded. Finally, sudden decreases of pH and increases of CO_2 were observed, lasting 1 or 2 min and occurring mainly upon first encounters between coral tissue and microsensors. We attributed this to firing of tentacle cells in response to irritation caused by the microsensor tip.

Experiments without inhibitors

Light and dark profiles

The concentration profiles of O_2, Ca^{2+} and CO_2 were strongly influenced by light (Fig. 1). During illumination (500 µmol photons m^{-2} s^{-1}), the O_2 concentrations at the polyp surface were ca 2.5× over-saturated (500 µM), CO_2 was depleted, and Ca^{2+} was ca 400 µM below the concentration of seawater. Consequently, in the light the polyp produced O_2, and consumed CO_2 and Ca^{2+}. In the dark, O_2 was almost depleted at the polyp surface (ca 40 µM), CO_2 was 95 µM (ca 9× higher than seawater) and Ca^{2+} was ca 400 µM above the concentration in seawater. Thus, in the dark the polyps

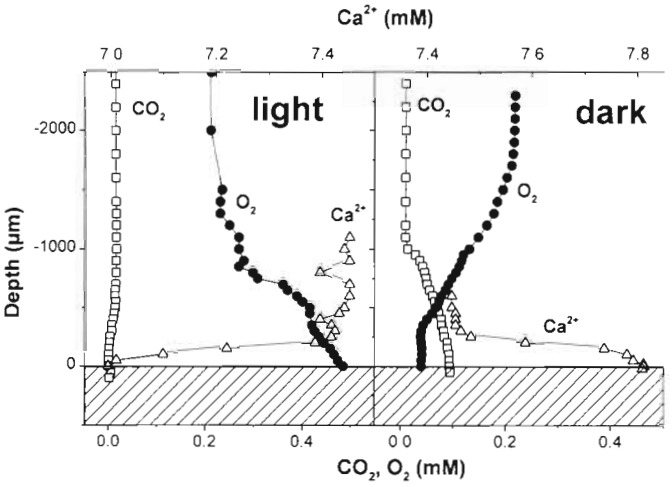

Fig. 1. *Favia* sp. Profiles of Ca^{2+} (△), O_2 (●) and CO_2 (□) in light and dark incubations. Dark profiles were measured 15 min (Ca^{2+}), 30 min (O_2) and 60 min (CO_2) after darkening, respectively

consumed O_2, produced CO_2 and excreted Ca^{2+}, at least during the experimental dark periods of up to 60 min. All profiles show the presence of a highly variable boundary layer adjacent to the polyp surface with a thickness of 200 to 1500 µm.

Heterogeneity of profiles

The oxygen distribution over the polyp surface, plotted in 2-D for 3 different flow velocities (Fig. 2), shows a strong heterogeneity of the oxygen distribution over the irregular polyp surface topography. Increased flow velocity decreases the thickness of the boundary layer and thus the concentration differences between seawater and polyp surface. Fig. 2 also illustrates that the coral tissue changes shape over time.

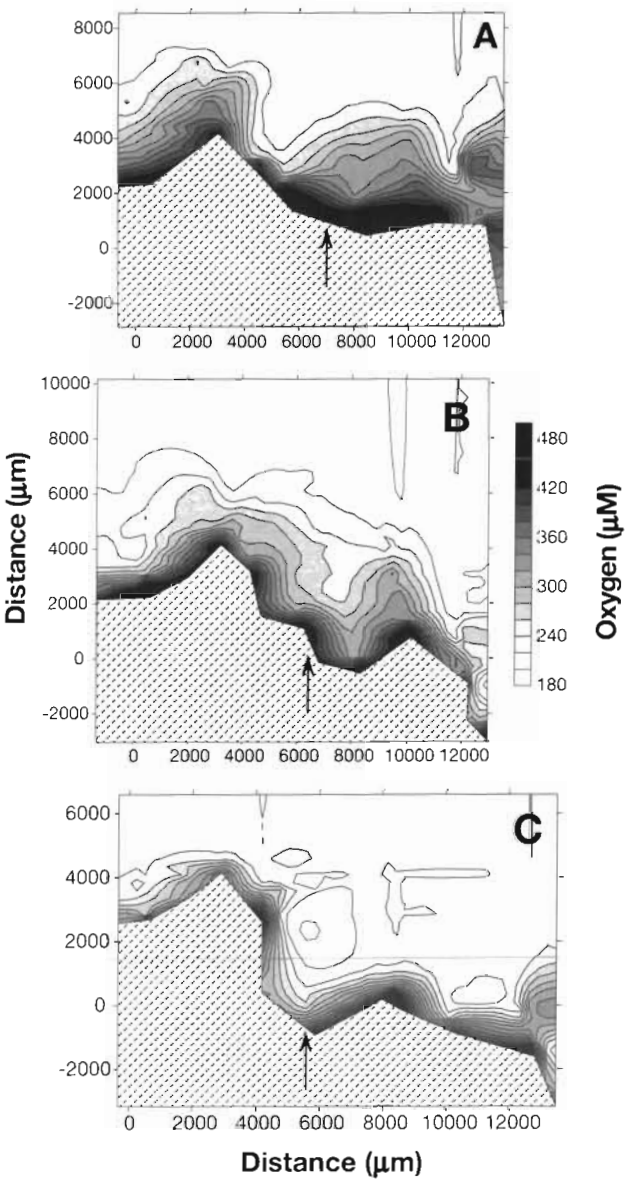

Fig. 2. *Favia* sp. Oxygen distribution over polyp surface at a flow velocity of (A) 1 cm s^{-1}, (B) 5 cm s^{-1} and (C) 10 cm s^{-1}. Dashed area: coral body. Arrows: position of the polyp mouth

O_2, CO_2, pH and Ca^{2+} concentration changes

O_2 and Ca^{2+} concentrations at the tissue surface responded immediately to experimental changes in light conditions (Fig. 3). When illuminated after a dark period, the O_2 concentration increased due to photosynthesis, and the Ca^{2+} concentration decreased. Reversibly, upon subsequent darkening O_2 decreased

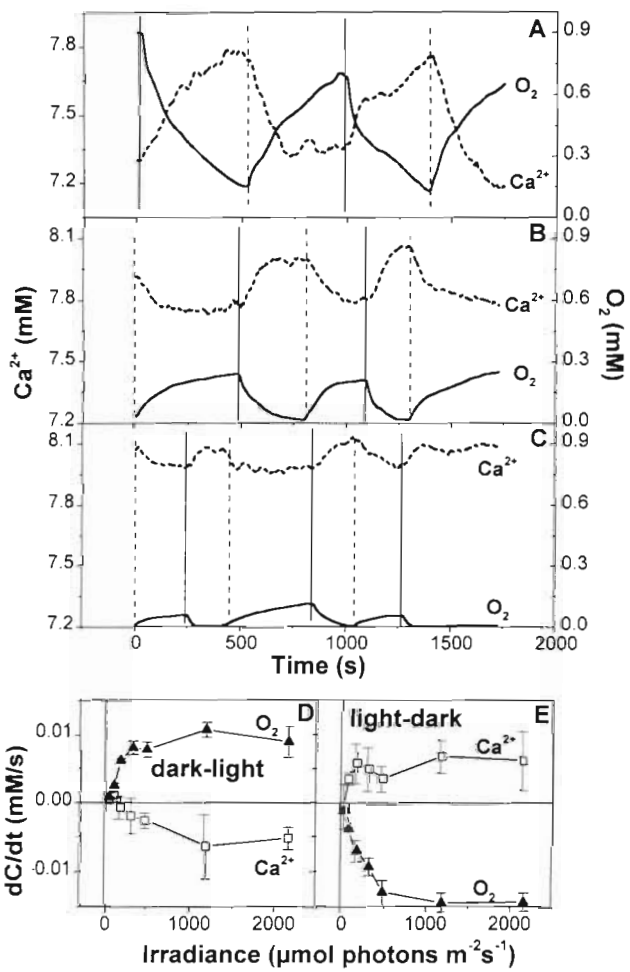

Fig. 3. *Favia* sp. Dynamics of O_2 (——, ▲) and Ca^{2+} (-----, □) at the polyp surface upon experimental dark-light and light-dark shifts, as a function of irradiance (510, 230 and 70 µmol photons m^{-2} s^{-1} for A, B and C, respectively). Vertical solid lines: light was switched off; vertical dashed lines: light was switched on. (D, E) Initial concentration changes upon (D) dark-light and (E) light-dark shifts as a function of irradiance (symbols with error bars: averages and standard deviations of 4 to 6 measurements)

and Ca^{2+} increased (Fig. 3A–C). The initial rates were about twice as high for O_2 as for Ca^{2+} (Fig. 3D, E), the amplitudes of the response curves of both compounds were similar (Fig. 3A–C). Typically, for the O_2 and Ca^{2+} dynamics the response curves were shaped like exponential rise functions for which the initial rates were the highest (see also Fig. 5). The rates of O_2 changes were higher upon a light-dark shift than a dark-light shift (see also Fig. 8). Although less clear, the Ca^{2+} dynamics also exhibited this phenomenon, especially at lower light intensities.

The pH and CO_2 showed slower and much smaller responses to changes in light regime

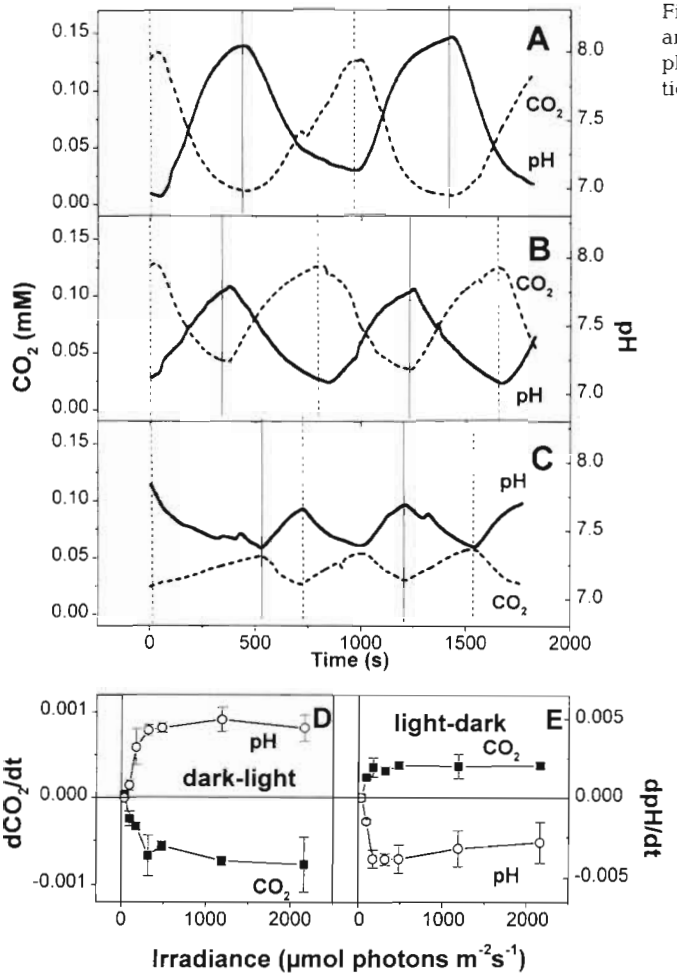

Fig. 4. *Favia* sp. Dynamics of pH (——, ○) and CO_2 (-----, ■) upon experimental dark-light and light-dark shifts, as a function of irradiance (481, 174 and 94 µmol photons m^2 s^{-1} for A, B, and C, respectively). Vertical solid lines: light was switched off; vertical dashed lines: light was switched on. (D, E) Maximal concentration changes upon (D) dark-light and (E) light-dark shifts as a function of irradiance (symbols with error bars: averages and standard deviations of 4 to 6 measurements)

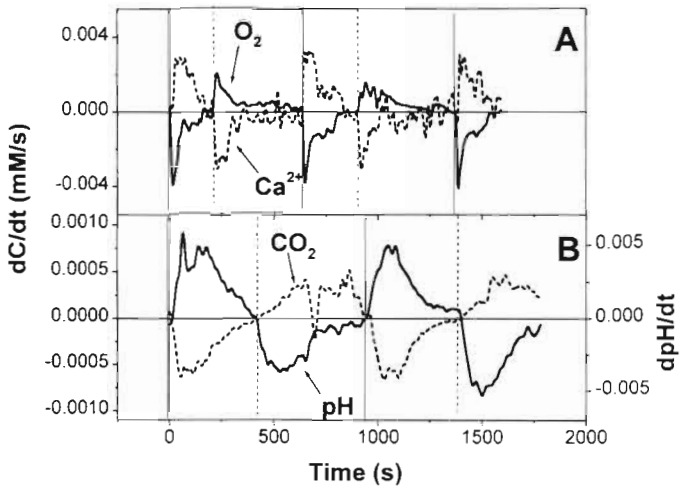

Fig. 5. *Favia* sp. Comparison of the dynamics of (A) O_2 (——) and Ca^{2+} (-----) and (B) pH (——) and CO_2 (-----). Dynamics are plotted as rates of concentration change, instead of concentrations. Vertical solid lines: light was switched off, vertical dashed lines: light was switched on

(Fig. 4). Upon illumination the pH increased and the CO_2 concentration decreased, and the opposite happened after darkening. However, upon darkening it took from seconds up to half a minute before an effect was observed on the pH and CO_2 concentration, and the maximum rates of concentration change were observed several minutes after darkening. Upon illumination after a dark period the pH and CO_2 concentrations showed a faster response than upon a light-dark shift; however, it took again minutes for the response to speed up to maximum rates. Consequently, the response curves were more shaped as sigmoidal curves with the largest rates in the middle. Since the initial rates were usually zero, in Fig. 4 the maximum response rates are plotted, not the initial rates. The amplitude of the response curve was smaller for CO_2 than for O_2 and Ca^{2+}. The difference between O_2/Ca^{2+} and CO_2/pH dynamics is more pronounced in Fig. 5, where the d*C*/d*t* (i.e. the change in the concentrations) instead of concentrations are plotted against time. The highest d*C*/d*t* for O_2/Ca^{2+} occurred directly after a change in illumination. After a change in illumination the d*C*/d*t* for CO_2/pH was initially low, increased for 30 s to several minutes and then decreased again.

Distribution of Ca^{2+} dynamics and gross photosynthesis

The gross photosynthesis and the Ca^{2+} concentration changes upon illumination were measured along a transect across a polyp. Both measurements

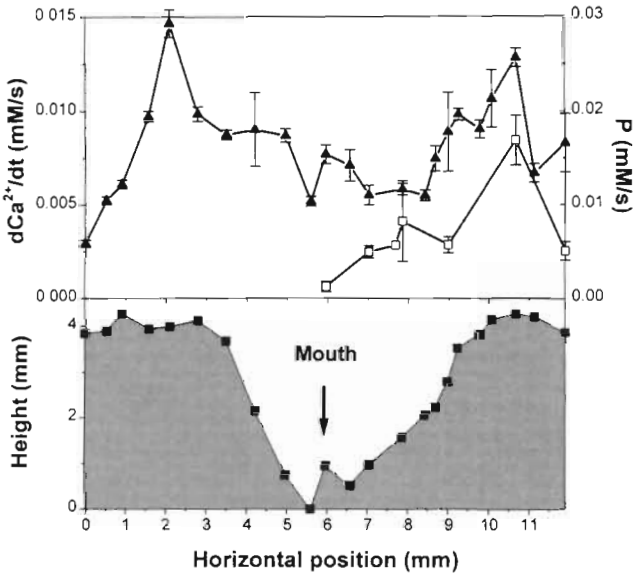

Fig. 6. *Favia* sp. Distribution of photosynthetic activity, P, (▲) and Ca^{2+} dynamics (□), over the coral surface (symbols with error bars represent averages and standard deviations of 3 to 5 measurements). Lower graph shows the shape of the polyp (shaded area) as determined from the positions where the microsensor was touching the surface (■). Arrow indicates the position of the polyp mouth opening

were performed on the same polyp under identical conditions. The dynamics of the Ca^{2+} concentrations (initial uptake rates) were most pronounced at the rim of the polyps and were lowest in the central region near the mouth (Fig. 6). This coincided accurately with the distribution of gross photosynthetic activity.

Effect of inhibitors

Ruthenium-red, an inhibitor of Ca-ATPase (Marshall 1996a), had no effect on photosynthesis, O_2 and Ca^{2+} dynamics, or on the Ca^{2+} profiles, even at concentrations of up to 100 µM, i.e. 5 times the recommended concentration (Marshall 1996a) (data not shown).

The effect of 2.5 µM DCMU on both the Ca^{2+} and O_2 surface concentration is demonstrated in Fig. 7. After DCMU addition to the recirculation tank, it took ca 15 min before inhibition was detected. Then it instantly reduced the O_2 concentration and increased the Ca^{2+} concentration, almost simultaneously. Photosynthesis was completely inhibited and both the O_2 and Ca^{2+} concentrations at the tissue surface stopped responding to light. The Ca^{2+} profile in light after DCMU treatment was similar to the dark profiles. Addition of 0.5 µM DCMU induced the same simultaneous effects on the Ca^{2+} and O_2 surface concentrations, and complete, although slower, inhibition of photosynthesis and Ca^{2+} dynamics (data not shown).

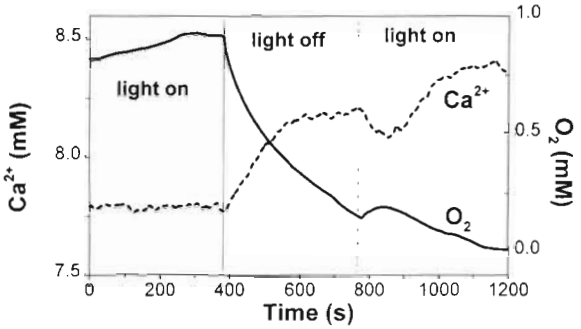

Fig. 7. *Favia* sp. Effect of DCMU (a photosynthesis inhibitor) on the O_2 (——) and Ca^{2+} (-----) surface concentrations. DCMU was added at $t = 0$ and became effective after ca 850 s. Vertical solid line: light was switched off; vertical dashed line: light was switched on

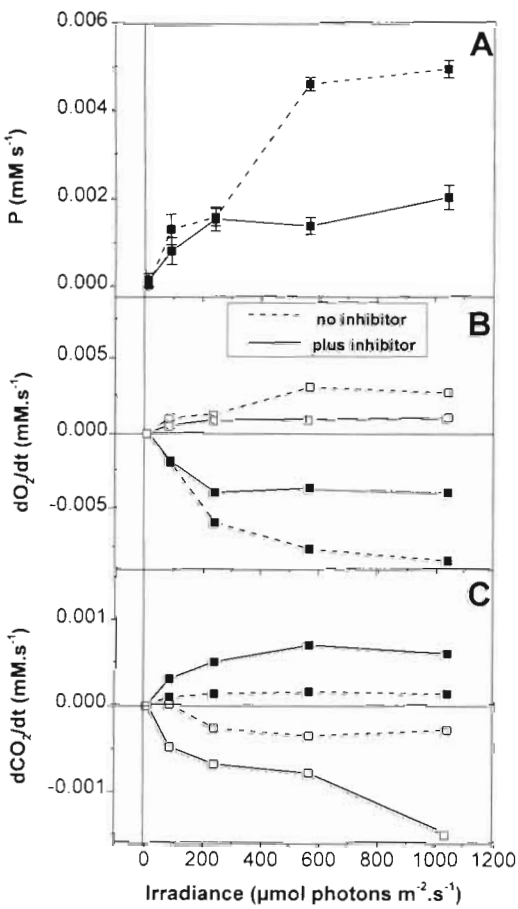

Fig. 8. *Favia* sp. Effect of ethoxyzolamide (a carbonic anhydrase inhibitor) on (A) the photosynthetic rates, measured with the fast light-dark method, (B) the maximal concentration changes of O_2 and (C) the maximal concentration changes of CO_2, at different light intensities. (——) Inhibitor added, (-----) no inhibitor added, (□) light-dark shift, (■) dark-light shift. The inhibitor was added at least 2 h before the measurements

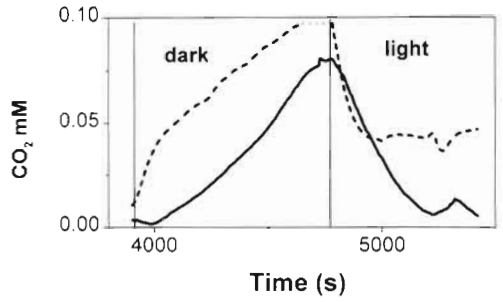

Fig. 9. *Favia* sp. Effect of ethoxyzolamide (inhibitor carbonic anhydrase) on CO_2 dynamics. (-----) Inhibitor added, (——) no inhibitor added. The inhibitor was added ca 2 h before the measurements

Ethoxyzolamide, an inhibitor of carbonic anhydrase, had an inhibitory effect on the gross photosynthesis rate. As shown in Fig. 8A, this was especially the case at higher light intensities. Similarly, the O_2 concentration changes upon light-dark and dark-light shifts, measured within the first 20 s instead of 1 s for gross photosynthesis, were inhibited at higher light intensities (Fig. 8B). Contrary to its effect on O_2 dynamics, the inhibitor stimulated the dynamics of CO_2 drastically (Figs. 8C & 9). After addition of ethoxyzolamide the CO_2 concentration at the polyp surface increased gradually in the course of the experiment (Fig 10). Unfortunately, the effect of ethoxyzolamide on the dynamics of Ca^{2+} and pH could not be measured reliably, due to excessive mucus formation by the polyp during this experiment.

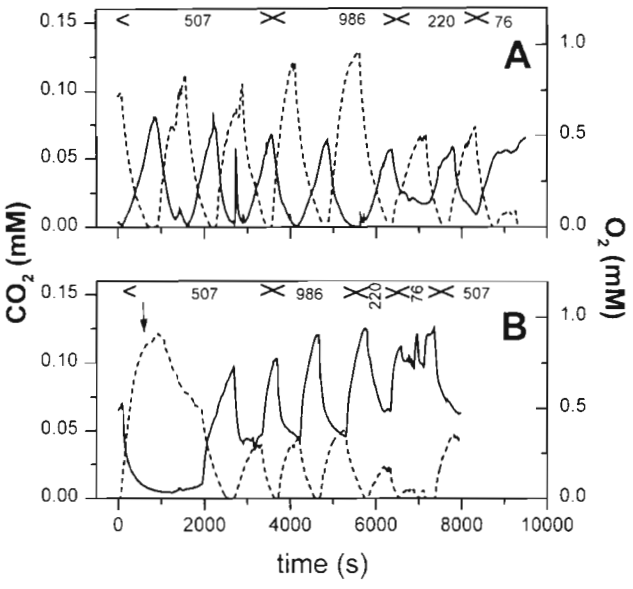

Fig. 10. *Favia* sp. Complete course of experiments where simultaneous O_2 (-----) and CO_2 (——) concentrations at the polyp surface were measured, showing the increase of CO_2 concentration upon carbonic anhydrase addition. Switches in illumination are not indicated. (A) without addition of inhibitor, and (B) with addition of ethoxyzolamide (inhibitor carbonic anhydrase); the inhibitor addition is indicated with an arrow. Numbers in the plots indicate the prevailing irradiance (μmol photons m^2 s^{-1})

DISCUSSION

Coral microenvironment

The measured microprofiles showed the presence of a diffusive boundary layer (DBL) that varied between 200 and 1000 μm in thickness (Fig. 1). The variation in boundary layer thickness is primarily due to the complex interaction between water flow and the irregular polyp topography. The distribution of oxygen over the polyp surface varied strongly and was dependent on the hydrodynamic regime (Fig. 2) in line with results of earlier DBL studies in corals (Patterson 1992, Shashar 1993, Kühl et al. 1995). The oxygen distribution data also illustrate that, due to the effect of the irregularity of the polyp surface on the profiles, the microprofiles cannot be used for flux calculations (for which a 1-D geometry is assumed; Kühl et al. 1995). Consequently, in order to compare the signal of 2 sensors, measurements must be done at close proximity. The O_2 profiles were similar to those measured previously (Kühl et al. 1995). Our measurements showed the presence of a very dynamic chemical microenvironment at the coral surface. In the light O_2 was produced and the coral took up CO_2 and Ca^{2+}, while the reverse was observed under dark incubation. A H^+ flux towards the coral tissue was observed in the light and an efflux to the seawater in the dark, probably due to photosynthesis- and respiration-induced shifts in the carbonate system. Our observations are in line with an earlier study of the coral microenvironment (Kühl et al. 1995) but provide new, and to our knowledge the first, data on Ca^{2+} and CO_2 dynamics in comparison with O_2 and pH dynamics measured at high spatio-temporal resolution.

Ca^{2+} and O_2 concentration changes

The dynamics of Ca^{2+} and O_2 were similar in amplitude and initial rates, but in opposed direction (Fig. 3). The initial concentration changes at the polyp surface are determined by the local uptake and production rates. The initial rates for O_2 were about twice as high for Ca^{2+}, thus approximately 1 Ca^{2+} is taken up per 2 O_2 molecules produced. The amplitudes of the O_2 and Ca^{2+} dynamics (the concentration difference between light and dark situation in steady state) is also determined by the transport through the DBL and thus by the diffusion coefficients. Since O_2 diffuses 2 to 3 times

faster than Ca^{2+}, and the amplitudes were approximately similar, this also shows a stoichiometry where 1 Ca^{2+} is taken up per 2 O_2 molecules produced.

The initial rates and amplitudes of the O_2 and Ca^{2+} dynamics increased with irradiance and exhibited a similar saturation curve (Fig. 3D, E). Together with the notion that the changes were simultaneous (Figs. 3A–C & 5), this indicates that both processes are tightly coupled, or that both are directly regulated by light. Also the equal distribution patterns of photosynthesis and Ca^{2+} dynamics within a single polyp points to a direct coupling between photosynthesis and Ca^{2+} uptake.

CO_2 and pH dynamics

The response of CO_2 concentrations and pH to light was much slower than that of O_2 and Ca^{2+}. This cannot be attributed to the slower sensors, as although the final signal level is reached after ca 10 s, both CO_2 and pH microsensors respond immediately to a concentration change. Often it was observed that the trend preceding a switch in illumination continued for seconds to minutes. This might suggest that the CO_2 transport across the polyp surface is only indirectly coupled to photosynthesis and respiration. However, both the carbonate system and the pH determine the CO_2 concentration changes, especially in the presence of the enzyme carbonic anhydrase that accelerates the conversion between CO_2 and HCO_3^- (Stumm & Morgan 1981). While respiration, photosynthesis and calcification determine the size of the dissolved inorganic carbon pool in and near the coral, the pH is determined by many other processes, e.g. proton pumps and membrane transport. We suppose that these processes contribute to the pH change directly after a light switch and that this in turn affects the CO_2 concentration, mediated by carbonic anhydrase at or near the polyp surface.

Assuming equilibrium, the total carbonate concentration ($CO_2 + H_2CO_3 + HCO_3^- + CO_3^{2-}$) can be calculated from the pH and the CO_2 concentrations, using known equilibrium constants. This calculation, applied to our simultaneous pH and CO_2 measurements during light-dark cycles, would result in a total carbonate concentration at the polyp surface varying between values close to zero under illumination to over 5 mM during darkness. As such extreme variations are impossible, and certainly cannot be attributed to respiration or photosynthesis, the basic assumption of the calculation is not valid: the CO_2 concentration at the polyp surface is not in equilibrium with the carbonate system, even in the presence of active carbonic anhydrase. The CO_2 concentration at the polyp surface is lower in the light than the equilibrium concentration and higher in the dark. Disequilibrium of the carbonate system was observed previously in microbial mats and biofilms with high photosynthetic and respiratory activities, and the phenomena observed were discussed in detail (de Beer et al. 1997). The low CO_2 level at the surface indicates that CO_2 is preferentially taken up by the polyp over other DIC components, e.g. by a CO_2 concentrating mechanism (Badger et al. 1980), which was indeed demonstrated in dinoflagellates (Berman Frank et al. 1994). However, there is evidence that polyps also actively take up HCO_3^- to supply symbiont photosynthesis (Goiran et al. 1996).

Comparison of all dynamics

The fast calcium dynamics were unexpected, as we assumed calcium dynamics at the surface to be a consequence of increased calcification by photosynthesis. The calcifying site is ca 1 mm below the surface, while photosynthesis takes place much closer to the tissue surface. We expected the following sequence of events upon illumination: (1) CO_2 to be fixed by photosynthesis, (2) the pH to increase in the photosynthetic zone (rather slowly, as our measurements show), (3) this pH increase to gradually expand to the calcifying zone near the skeleton, (4) the pH increase will lead to increased calcification and thus a decrease of the local Ca^{2+} concentration, which (5) will eventually result in a Ca^{2+} decrease at the polyp surface. This mechanism will lead to very slow and delayed Ca^{2+} concentration changes at the surface, certainly slower than the pH change. However, the opposite was observed. Thus, the observed Ca^{2+} dynamics at the surface cannot be explained by calcification mediated through a photosynthetically driven pH increase. The data indicate a coupling between pH and CO_2, and between Ca^{2+} and O_2. The differences in dynamics between CO_2/pH and Ca^{2+}/O_2 surface concentrations are not consistent with the view that Ca^{2+} uptake is regulated by pH changes induced by photosynthesis (McConnaughey 1987, Carlon 1996, Goreau et al. 1996). Instead, a more direct coupling between photosynthesis and Ca^{2+} exchange can explain the data.

A remarkable phenomenon is the higher O_2 concentration change after switching off the light than upon illumination after a period of darkness. The same was observed for Ca^{2+} dynamics. The opposite was found for the dynamics of CO_2 and pH that were higher upon illumination than upon darkening. However, the dynamics of CO_2/pH and O_2/Ca^{2+} (Figs. 3D, E & 4D, E) are not quite comparable, as for the CO_2/pH, not the initial rates (they were usually zero) but the highest rates were plotted. Similar observations were previously (Kühl et al. 1995) reported on pH and O_2 dynam-

ics in corals, but in planktonic symbiont bearing foraminifera no significant difference was observed between light-dark and dark-light O_2 dynamics (Rink et al. 1998). An explanation of these phenomena may be important for the understanding of the coupling between photosynthesis and respiration in photosynthesizing communities. The dynamics are a result of the sum of various host and symbiont respiration processes and photosynthesis. The accumulation of reduced pools and excretion of photosynthates by symbionts are important for the respiration of the host. Phenomena such as light and dark respiration and the post-illumination burst of respiration determine oxygen consumption by the symbionts. Furthermore, the regulation of the photosynthesis by RuBisCo, which catalyses both O_2 and CO_2 fixation, must be considered. Which of both processes prevails is determined by the local O_2/CO_2 ratio: when it is low CO_2 is fixed, when it is high O_2 is fixed. Our data cannot be conclusive on this matter, as the O_2/CO_2 ratio at the RuBisCo site may considerably differ from the polyp surface concentration, due to the carbon concentration mechanism. A comprehensive discussion of these processes in micro-algae has been published previously (Beardall & Raven 1990).

Effect of inhibitors

Inhibition of carbonic anhydrase inhibited photosynthesis at higher light intensities and increased the CO_2 dynamics under all experimental conditions (Figs. 9 & 10) . This can be explained by the notion that actually CO_2 is the primary substrate for photosynthesis at the level of RuBisCo, the enzymatic site of CO_2 fixation. Carbonic anhydrase catalyses the reversible conversion of CO_2 to HCO_3^- and, thereby, brings the CO_2 concentration faster in equilibrium with the pH and the carbonate pool. Thus, in a dynamic situation where the carbonate system components and H^+ are in a temporal or spatial concentration change, the action of carbonic anhydrase will bring the CO_2 concentration closer to the equilibrium concentration (de Beer et al. 1997). Since the carbonate pool is much larger than the CO_2 concentration, this mechanism effectively buffers the CO_2 concentration. Inhibition of carbonic anhydrase uncouples the CO_2 from the carbonate pool, since the non-catalyzed reaction to and from HCO_3^- is slow. Thus the supply to RuBisCo is strongly reduced, resulting in a fast CO_2 decrease during illumination. Conversely, in the dark the conversion of CO_2, formed by respiration, to HCO_3^- is reduced as well, resulting in accumulation. Because the inhibitor uncouples CO_2 to some extent from the carbonate pool, inhibition of carbonic anhydrase brings the CO_2 and O_2 dynamics closer to stoichiometry. However, when carbonic anhydrase is inhibited, the CO_2 dynamics upon illumination are higher than upon darkening, the opposite as observed for O_2.

The inhibition of carbonic anhydrase resulted in a decrease of the photosynthesis rate at higher light intensities. This can be understood from the decreased supply of CO_2 to the RuBisCo enzyme. CO_2 is supplied to the symbionts by diffusion from the seawater, by respiration from the polyp and from the carbonate pool. If carbonic anhydrase is inhibited, the supply from the carbonate pool is strongly reduced. At low light intensities the supply of CO_2 by transport (from the seawater and respiratory zones) and non-catalyzed conversion of HCO_3^- is sufficient. However, at higher light intensities, and thus at higher photosynthetic capacity, CO_2 supply from the carbonate pool and transport from the polyp tissue limits the photosynthetic rate. This CO_2 limitation must be a local phenomenon: during exposure to carbonic anhydrase inhibitor the CO_2 concentration at the polyp surface increases significantly (Fig. 10). Even during illumination, CO_2 surface concentrations exceed seawater levels. This indicates that carbonic anhydrase plays a crucial role in the transport of CO_2 to the RuBisCo enzyme, on the level of the cell membrane or the chloroplasts, i.e. an inorganic carbon concentrating mechanism. The inhibitor we used can penetrate into cells and thus inhibited all carbonic anhydrase present. The carbonic anhydrase inhibitor DIAMOX, not used in this study, does not penetrate cells (Goiran et al. 1996). The use of both inhibitors may be useful to differentiate between the activities of intracellular and extra-cellular carbonic anhydrase and their relevance to photosynthesis.

Since Ruthenium-red had no effect on the Ca^{2+} dynamics, an ATPase does apparently not mediate Ca^{2+} uptake at the surface of *Favia* sp. The reported reduction of coral calcification by this inhibitor (Marshall 1996a) indicates a role of Ca-ATPase in the Ca^{2+} transport through the tissue or extrusion of Ca^{2+} at the skeleton site (Ip et al. 1991).

The simultaneous inhibition of Ca^{2+} and O_2 dynamics by the photosynthesis inhibitor DCMU strongly indicates that Ca^{2+} concentration dynamics at the tissue surface are directly regulated by photosynthesis and not by light. Since the Ca^{2+} dynamics were not simultaneous with the pH/CO_2 dynamics, it is highly unlikely that they are linked mechanistically in a direct way.

In conclusion we have shown that (1) the spatial distribution of calcium dynamics and oxygen dynamics are similar, (2) the magnitude and time constants of the calcium dynamics and oxygen dynamics are similar, and (3) that both dynamics are simultaneously inhib-

ited by DCMU. This points to a very strong relationship between processes ruling these dynamics. This is the basis of our speculation on the existence of a calcium uptake mechanism directly regulated by photosynthesis.

These experiments do not elucidate the mechanism of Ca^{2+} uptake regulation by photosynthesis. Since the intracellular Ca^{2+} concentration is maintained at submicromolar levels (Chalker et al. 1983), and the concentration in seawater is ca 8 mM, uptake into the cytoplasm could, e.g., be regulated by a gated channel activated by photosynthesis. It is puzzling that the Ca^{2+} profiles, measured in the dark and upon exposure to DCMU, indicate export of calcium from the tissue in the absence of photosynthesis. This phenomenon needs clarification and further experiments are planned. It is thought that Ca^{2+} transport through the tissue occurs in separate compartments, such as specialized vesicles (Johnston 1980). Another study suggested more complicated combination of serial and parallel calcium transport mechanisms through a number of tissue and skeleton associated pools (Tambutte et al. 1996). In uptake experiments 3 pools were found: 1 associated with tissue and 2 associated with the skeleton; in efflux experiments 2 tissue associated pools were distinguished and again 2 skeleton-associated pools were found. The tissue-associated pools were ca 7 nmol mg^{-1} protein, resulting in an average Ca^{2+} tissue concentration of ca 1 mM (Tambutte et al. 1996). Since this is lower than the surrounding seawater, the observed efflux from the tissue can be explained by (1) active transport (by a Ca-ATPase) or (2) by the presence of a tissue-associated compartment with a Ca^{2+} concentration higher than seawater. Since the cytoplasm concentration is sub-micromolar (Chalker et al. 1983), and efflux from the tissue is not influenced by Ca-ATPase inhibitor Ruthenium-red, it seems most likely that indeed tissue-associated compartments exist with a high Ca^{2+} concentration, such as the specialized vesicles mentioned above (Johnston 1980). Detailed studies on the formation and behavior of such vesicles might lead to more profound insight into calcification processes.

The photosynthetic symbionts are positioned less than 50 µm from the polyp surface (Barnes & Chalker 1990). This geometry would facilitate regulation of calcification by photosynthesis on the level of Ca^{2+} uptake rather than on the more remote sites of Ca^{2+} secretion and calcification. However, Ca^{2+} is taken up by polyp tissue, not by the symbiotic algae. It is known that the host can enhance the CO_2 fixation and induce the secretion of photosynthate from its symbionts by chemical agents, known generically as 'host factors' (Muscatine 1967, Gates et al. 1995). Our results indicate that the symbionts can also regulate Ca^{2+} exchange of the host. Of course, calcification has been demonstrated in the dark, and occurs in ahermatypic corals (Marshall 1996a). However, our data do not exclude the possibility that several calcium uptake and calcification mechanisms exist and operate in parallel. The regulation of calcium uptake by photosynthesis allows corals to fine-tune the calcification rates according to environmental constraints, and to counterbalance increasing pH in the light due to photosynthesis.

Acknowledgements. We thank Gaby Eickert for technical assistance, Andrea Wieland and Prof. Z. Dubinsky (Bar Ilan University) for critically reviewing the manuscript, and Prof. A. W. D. Larkum (University Sidney) for valuable advice. The Red Sea Program (Project E: 'Microbial activities at marine interfaces controlling sediment-water fluxes'), financed by the German Ministry for Research and Development (BMBF), supported the work.

LITERATURE CITED

Ammann D, Bührer T, Schefer U, Müller M, Simon W (1987) Intracellular neutral carrier based Ca^{2+} microsensor with sub-nanomolar detection limit. Pflügers Arch 409:223–228

Badger MR, Kaplan A, Berry JA (1980) Internal carbon pool of *Chlamydomonas reinhardtii*. Plant Physiol 66:407–413

Barnes DJ, Chalker BE (1990) Calcification and photosynthesis in reef-building corals and algae. In: Dubinsky Z (ed) Coral reefs. Elsevier, Amsterdam, p 109–131

Beardall J, Raven JA (1990) Pathways and mechanisms of respiration in microalgae. Mar Microb Food Webs 4(1):7–30

Berman Frank I, Zohary T, Erez J, Dubinsky Z (1994) CO_2 availability, carbonic anhydrase, and the annual dinoflagellate bloom in Lake Kinneret. Limnol Oceanogr 39(8):1822–1834

Broecker WS, Peng TH (1974) Gas exchange rates between air and sea. Tellus 26(1-2):21–35

Carlon DB (1996) Calcification rates in corals. Science 274:117

Chalker BE, Dunlap WC, Oliver JK (1983) Bathymetric adaptation of reef-building corals at Davies Reef, Great Barrier reef, Australia. II Light saturation curves for photosynthesis and respiration. J Exp Mar Biol Ecol 73:37–56

Crossland CJ, Barnes DJ (1974) The role of metabolic nitrogen in coral calcification. Mar Biol 28:187–195

de Beer D, Glud A, Epping E, Kühl M (1997) A fast responding CO_2 micro-electrode for profiling sediments, microbial mats and biofilms. Limnol Oceanogr 42(7):1590–1600

Erez J (1983) Calcification rates, photosynthesis and light in planktonic foraminifera. In: Westbroek P, de Jong EW (eds) Biomineralization and biological metal accumulation. Biological and Geological Perspectives, D. Reidel Publishing Company, Dordrecht, p 307–312

Gao K, Aruga Y, Asada K, Ishiara T, Akano T, Kiyohara M (1993) Calcification in the articulated coralline alga *Corallina pilulifera*, with special reference to the effect of elevated CO_2 concentration. Mar Biol 117:129–132

Gates RD, Hoegh-Guldberg O, McFall-Ngai MJ, Bil KY (1995) Free amino acids exhibit anthozoan 'host factor' activity: they induce the release of photosynthate from symbiotic dinoflagellates *in vitro*. Proc Natl Acad Sci 92: 7430–7434

Gattuso JP, Allemand D, Michel F (1999) Photosynthesis and calcification at cellular, organismal and community levels in coral reefs: a review on interactions and control by carbonate chemistry. Am Zool 39:160–183

Glud RN, Ramsing B, Revsbech NP (1992) Photosynthesis and photosynthesis-coupled respiration in natural biofilms quantified with oxygen microsensors. J Phycol 28:51–60

Goiran C, Al Moghrabi S, Allemand D, Jaubert J (1996) Inorganic carbon uptake for photosynthesis by the symbiotic coral/dinoflagellate association. I. Photosynthetic performances of symbionts and dependence on seawater. J Exp Mar Biol Ecol 199(2):207–225

Goreau TF, Goreau NI (1959) The physiology of skeleton formation in corals. II. Calcium deposition by hermatypic corals under various conditions in the reef. Biol Bull 117: 239–250

Goreau TJ, Goreau NI, Trench RK, Hayes RL (1996) Calcification rates in corals. Science 274:117

Ip YK, Krisnaveni P (1991) Incorporation of strontium ($^{90}Sr^{2+}$) into the skeleton of the hermatypic coral *Galaxea fascicularis*. J Exp Zool 258:273–276

Ip YK, Lim ALL, Lim RWL (1991) Some properties of calcium-activated adenosine triphosphatase from the hermatypic coral *Galaxea fascicularis*. Mar Biol 111:191–197

Jensen K, Revsbech NP, Nielsen LP (1993) Microscale distribution of nitrification activity in sediment determined with a shielded microsensor for nitrate. Appl Environ Microbiol 59(10):3287–3296

Johnston IS (1980) The ultrastructure of skeletogenesis in hermatypic corals. Int Rev Cyt 67:171–214

Kühl M, Cohen Y, Dalsgaard T, Jørgensen BB, Revsbech NP (1995) Microenvironment and photosynthesis of zooxanthellae in scleractinian corals studied with microsensors for O_2, pH and light. Mar Ecol Prog Ser 117:159–172

Li YH, Gregory S (1974) Diffusion of ions in sea water and deep-sea sediments. Geochim Cosmochim Acta 38: 703–714

Marshall AT (1996a) Calcification in hermatypic and ahermatypic corals. Science 271:637–639

Marshall AT (1996b) Calcification rates in corals. Science 274: 117–118

McConnaughey TD (1987) Biomineralization mechanisms. In: Crick RE (ed) Origin, evolution and modern aspects of biomineralization in plants and animals. Plenum Press, New York, p 57–73

McConnaughey TD (1991) Calcification in *Chara corallina*: CO_2 hydroxylation generates protons for bicarbonate assimilation. Limnol Oceanogr 36(4):619–628

McConnaughey TD (1994) Calcification, photosynthesis, and global carbon cycles. Bull Inst Oceanogr Monaco s13: 137–161

Muscatine L (1967) Glycerol excretion by symbiontic zooxanthellae from corals and *Tridacna* and its control by the host. Science 156:516–519

Muscatine L, Tambutte E, Allemand D (1997) Morphology of coral desmocytes, cells that anchor the calicoblastic epithelium to the skeleton. Coral Reefs 16(4):205–213

Patterson MR (1992) The impact of symbiosis on invertebrate physiology, ecology and evolution. A chemical engineering view of Cnidarian symbiosis. Am Zool 32(4):566–582

Pennisi E (1998) New treat seen from carbon dioxide. Science 279:989

Revsbech NP (1989) An oxygen microsensor with a guard cathode. Limnol Oceanogr 55:1907–1910

Revsbech NP, Jørgensen BB (1983) Photosynthesis of benthic microflora measured with high spatial resolution by the oxygen microprofile method: capabilities and limitations of the method. Limnol Oceanogr 28(4):749–756

Revsbech NP, Jørgensen BB (1986) Microsensors: their use in microbial ecology. Adv Microbial Ecol 9:293–352

Rink S, Kühl M, Bijma J, Spero HJ (1998) Microsensor studies of photosynthesis and respiration in the symbiontic foraminifer *Orbulina universa*. Mar Biol 131:583–595

Shashar N, Cohen Y, Loya Y (1993) Extreme diel fluctuations of oxygen in diffusive boundary layers surrounding stony corals. Biol Bull 185:455–461

Stumm W, Morgan JJ (1981) Aquatic chemistry, 2nd edn. John Wiley and Sons, New York

Tambutte E, Allemand D, Bourge I, Gattuso JP, Jaubert J (1995) An improved ^{45}Ca protocol for investigating physiological mechanisms in coral calcification. Mar Biol 122: 453–459

Tambutte E, Allemand D, Müller E, Jaubert J (1996) A compartmental approach to the mechanism of calcification in hermatypic corals. J Exp Biol 200:1029–1041

VanderMeulen JH, Davis ND, Muscatine L (1972) The effects of inhibitors of photosynthesis on zooxanthellae from corals and other invertebrates. Mar Biol 16:185–191

Yamashiro H (1995) The effects of HEPB, an inhibitor of mineral deposition, upon photosynthesis and calcification in the scleractinian coral, *Stylophora pistillata*. J Exp Mar Biol Ecol 191:57–63

Editorial responsibility: Otto Kinne (Editor), Oldendorf/Luhe, Germany

Submitted: February 19, 1999; Accepted: September 10, 1999
Proofs received from author(s): February 3, 2000